

# Analysis of the jam signal effect against the conical-scan seeker

Tsholofelo M. Malatji<sup>a,b</sup>, Warren P. du Plessis<sup>a</sup>, Cornelius J. Willers<sup>b</sup>

<sup>a</sup>University of Pretoria, Pretoria, South Africa, 0002

<sup>b</sup>Council for Scientific and Industrial Research, Pretoria, South Africa, 0001

**Abstract.** There remains a wide proliferation of second-generation frequency-modulated conical-scan seekers in the hands of irregular forces, while the understanding of what makes a jam signal effective remains unclear. It is generally known that the [jam-to-signal \(J/S\)](#) ratio, the jam signal frequency, and the duty cycle are the parameters that need consideration when developing an effective jam code, but the effect of using different jammer waveforms is not generally known. This study investigates the effect of using different jammer waveforms namely: the fixed carrier, low frequency, [amplitude modulation \(AM\)](#) and [frequency-modulation \(FM\)](#) jam codes, for jam signal analysis. Of the tested jam signals, it was found that the [AM](#) jam code is most effective in countering the conical-scan seeker due to the amplitude variations created by the jam signal.

**Keywords:** Jamming, jam code, jammer waveform, conical-scan, reticle, countermeasures.

\*Tsholofelo M. Malatji, [tmalatji@csir.co.za](mailto:tmalatji@csir.co.za)

## 1 Introduction

Since their invention in the 1960's, [Man-portable air-defence systems \(MANPADSs\)](#) have remained a threat to civilian and military aircraft due to a large number being unaccounted for. The United States government estimates that a few thousand [MANPADS](#) are outside of government controls.<sup>1</sup> It is also estimated that these weapons could easily be sold for as little as USD 1000 each, making these weapons easily accessible to non-government forces.<sup>1</sup> The majority of aircraft losses in major conflicts around the world have been attributed to [MANPADS](#) missiles especially first and second generation [MANPADS](#).<sup>2</sup> While there is a wide proliferation of first and second

generation missiles, there is a lack of open information on how to effectively counter these **MANPADS**. This information is restricted and classified due to security reasons but this is worrying in light of the danger these missiles pose to civilian aircraft.

Several types of **Infrared countermeasures (IRCM)** have been developed to defeat these missile threats.<sup>3</sup> These include **infrared (IR)** decoys such as flares and onboard devices known as jammers.<sup>4</sup> Flares provide an effective countermeasure against the early generation missiles, but they are less effective against modern missiles. Furthermore, their protection capability is compromised by the fact that only a limited number of flares can be carried on-board a platform.<sup>5</sup> An active jammer can be used repeatedly in subsequent engagements, flexibly using different jam codes to counter different missile threat types.

Much study has gone into the development of **Directed infrared countermeasure (DIRCM)** systems which can deliver jamming codes to the seeker optics with successful results.<sup>5</sup> A **DIRCM** jammer system creates **IR** pulse sequences that confuse the processor within the missile seeker and therefore create an illusion of a target.<sup>6</sup> Each missile type requires a potentially different jamming sequence, if one jam code is not effective, another must be tried.<sup>7</sup> Hence, the jammer pulse waveform must cause **optical break lock (OBL)** within a few hundred milliseconds to allow different codes' use. Advanced closed-loop **DIRCM** systems monitor the reflected jamming laser return signal from the seeker's optics (cat-eye effect). The return signal signature can be used to identify the type of seeker, allowing an optimal jam code selection. The return signal can also be used to determine the effectiveness of a specific jam code. A number of **DIRCM** systems have been developed and deployed in the recent years,<sup>5</sup> yet the open literature does not provide information about what makes a jammer signal successful.<sup>6,8-13</sup> For example, some sources suggest that the jammer frequency must be close to the target signal frequency to ensure jammer success,<sup>6,8-11,13</sup>

while others suggest that the jammer frequency is successful when it is twice the target signal frequency.<sup>12</sup>

The literature frequently reports on the effect of the required [jam-to-signal \(J/S\)](#) ratio. The general consensus seems to indicate that the jammer signal intensity must be much higher than the target intensity.<sup>6,8-13</sup> However, the required [J/S](#) ratio magnitude to ensure jammer success is not clear from the open literature. Some sources suggest that effective jamming requires physical imperfections or artefacts in a conical-scan seeker.<sup>6,7</sup> These imperfections are reported to include optical scattering and reflections, and vibration disturbance effects in the seeker. Optical scattering, and retro-reflection occurs in the missile seeker's optics producing spurious signals that confuse a missile's signal processing. There is a measure of coherence between the target signal chopped by the nutating image and the signal resulting from radiation scattering off the rotating optics. At the same time, there is also an asynchronous signal with apparently random phasing and amplitude resulting from the scattering from asymmetry in the optics and mechanical parts. This effect disturbs the frequency modulation of the detector signal and thereby induces errors in the tracking loop. The severity of the optical scattering effect increases with increasing jamming signal intensity. Although this effect is mentioned as critically important in evaluating jam signal effectiveness,<sup>6</sup> description of such models are not available in the literature.<sup>6,8-13</sup> The reason for not modelling optical scattering and vibration effects is that they result from a large number of real-world, compounded random defects in the optical materials, dust, scratches, manufacturing surface finish, tolerance errors, and components' design asymmetry. These effects cannot be modelled accurately by simple mathematical models.

This paper considers the matter of determining optimal deterministic jamming waveforms that would not rely on vibration or optical scattering effects. Such waveforms are known to exist.<sup>12,13</sup>

The majority of studies do not indicate what such jammer waveform should look like or whether different waveforms have an effect on jammer success.<sup>6,8-12</sup> The general consensus in the literature is that the jammer signal should be similar to the target signal for maximum jamming effectiveness. However, simple logic seems to indicate that a jamming signal that exactly matches the chopped target signal would emulate and enhance the target signal. The effect of the duty cycle at which a jam signal is operated is also rarely reported on.<sup>6,8-12</sup> This gives an impression that the effect of changing the duty ratio is not critical to the success of the jam signal. Hence, some clarification is required on the relevant jammer parameters and their effects on a seeker.

Effective missile-seeker jamming requires that the jam code be matched to the missile type. Determining and confirming the missile type during an operational mission is no simple task. The process of determining the missile type is typically performed under closed loop jamming. As an alternative to low-power jamming, [high-power lasers \(HPLs\)](#) have been considered for the purpose of destroying sensitive missile components. The use of a [HPL](#) would eliminate the need to identify and classify the missile seeker before administering a jam code.<sup>7</sup> The disadvantage of using [HPLs](#) is that the power required for this countermeasure is much higher than that required for jamming. This makes the use of [HPLs](#) impractical in many situations, such as on small platforms.<sup>7,14</sup>

This paper presents results of an investigation into the jamming of a [frequency-modulation \(FM\)](#) conical-scan missile seeker, attempting to address the lack of information on the required [J/S](#) ratio and jamming code signals in the open literature due to their classified nature. A criterion for jam effectiveness was defined and the signal parameters and jam codes that ensure jam success were determined. The discussion starts with a brief description of the operation of the conical-scan seeker in [Section 2](#), before moving on to a discussion of the jammer parameters that were tested and the results thereof in [Section 3](#). Finally, a brief conclusion is provided in [Section 4](#).

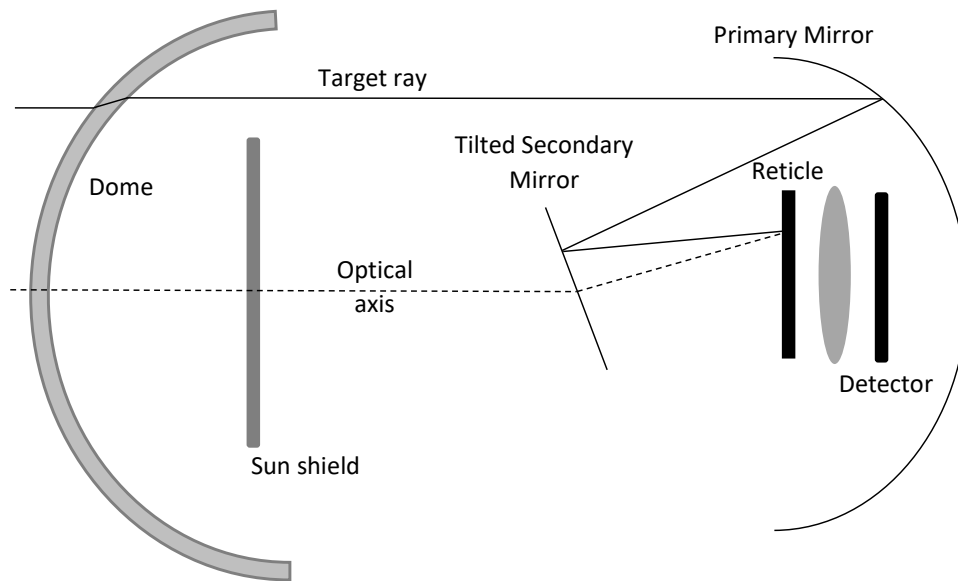


**Fig 1** Conical scan optics concept.

## 2 Conical-scan seeker signal processing

The conical-scan seeker typically consists of a primary mirror (rotationally stationary with respect to the object-space optical axis), a spinning tilted secondary mirror, and a stationary reticle as shown in Fig. 1. The tilt of the secondary mirror creates an offset of the target image on the reticle, bending the optical axis. As the secondary mirror rotates, the image-space optical axis offset rotates. This effect is called the nutation of the optical axis and effectively shifts the image on the reticle around the reticle centre. The trace of the object-space optical axis on the reticle is called the nutation circle. Note that the image remains upright as the image nutates as shown in Figs 2 (a) and 2 (c); the image moves, it does not rotate.

The radiation from the nutating scene falls onto the reticle, which comprises transparent and opaque regions in a well-designed pattern, often a variation of a simple wagon wheel shape, like that shown in Fig. 2.<sup>9,10,15-19</sup> As the scene image moves across the reticle, the signal from a small object in object space (the target) is chopped or modulated across the regions of different transparency in the reticle. The signal is detected as a sequence of pulses as the signal is chopped.

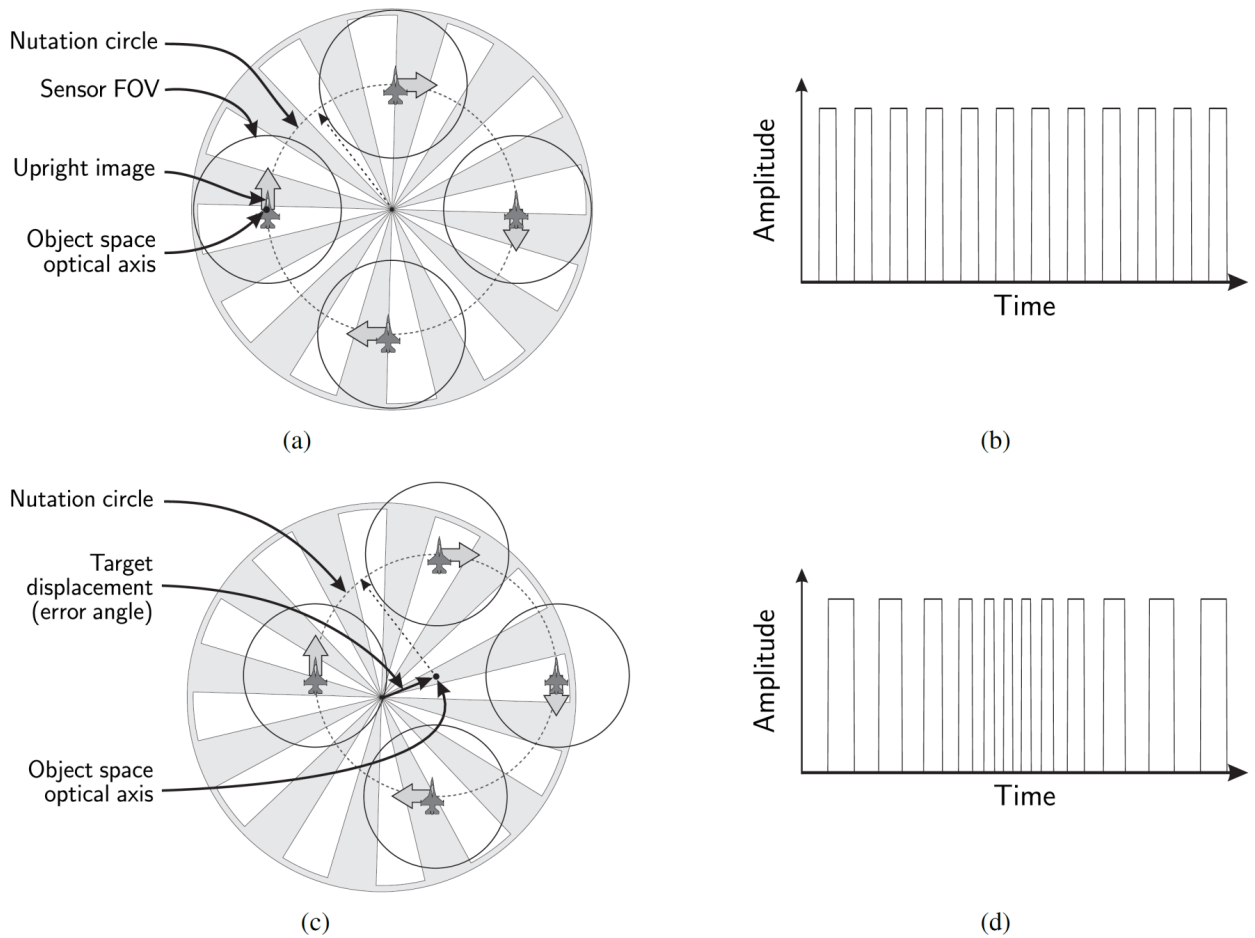


**Fig 2** Typical wagon wheel reticle (a) with no error, and (b) the associated detector signal, (c) the wagon wheel reticle with a nutation error and (d) the associated detector signal.

The target IR signature is constant over time with the modulation of the detector signal being solely a result of the reticle modulation. As a result, the signal from a target can be considered a fixed-carrier FM signal. Large objects (e.g. clouds) cover a large area on the reticle, several times the reticle spoke width, resulting in an averaging effect, called spatial filtering. The reticle's spatial filtering suppresses large objects in the image, but has smaller or no effect on point source targets. The detector is placed behind the reticle, converting the chopped IR signal to an electronic signal. The detector signal is processed to extract the target movement, which is then used to create a steering signal for the seeker.

The nutating movement of a small target spot in the image creates a frequency-modulated

signal, with the modulation index depending on the target displacement error angle relative to the optical axis.<sup>6,8-13</sup> For an on-axis small target, the nutation circle is centred on the reticle centre (see Fig. 2 (a)) and the FM modulation depth is zero (see Fig. 2 (b)). For an off-axis small target, the nutation circle shifts its centre away from the reticle centre (see Fig. 2 (c)), and the small target chopped signal has a non-zero modulation depth (see Fig. 2 (d)). The frequency-modulation depth can be used to determine the radial target displacement error angle, and the phase of the modulation signal envelope gives the angular position of the target. The target radial displacement error angle and rotational displacement angle can therefore be extracted from the signal by FM demodulation techniques.

When a target image moves near the reticle centre, the modulation frequency can become very high. Furthermore, it is not possible to practically realise the very small spoke widths near the centre of the reticle, with the result that the centre of the reticle loses reticle pattern resolution. For these reasons, the centre of the simple wagon wheel reticle is normally modified in practice to overcome these difficulties. However, a standard wagon wheel reticle was used in this investigation because the theoretical analysis is not significantly affected by these practical issues. In this study, the target image on the reticle is infinitesimally small and the spoke widths are not constrained by physical realisability, meaning that spatial chopping was effective very near the reticle centre, with no spatial filtering being observed. The nutation circle was thus allowed to move freely without constraint. By comparison, the nutation circle of a practical systems is generally not allowed to approach the centre of the reticle to limit the modulation index and avoid excessive spatial filtering. The simulation allowed for large modulation index when the target passed near the reticle centre. The simulation also did not have a constrained field of view, but this is irrelevant in the present study because there are no flares or background clutter sources (only the target signal is present).

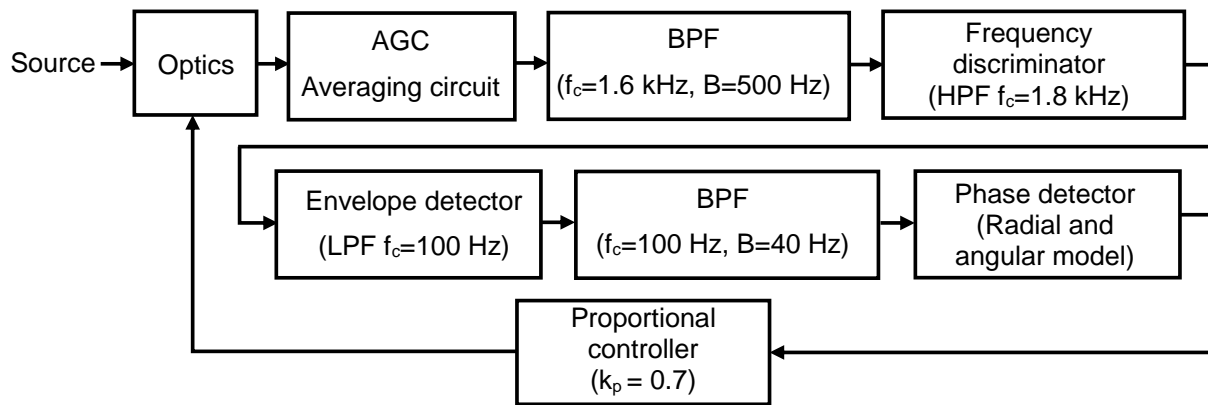


Fig 3 Signal processing block diagram.<sup>20</sup>

Despite this idealised representation, useful insight into the performance of practical seekers is still obtained as the range of modulation indices considered included those used by practical missile seekers.

Fig. 2 shows the sensor **field of view (FOV)** as a circle centred on the nutation circle. The sensor **FOV** must be smaller than the reticle radius to ensure that the entire sensor **FOV** is modulated by the reticle as the region outside the reticle radius is opaque. The total **FOV** was defined as the point at which the edge of the nutation circle touches the edge of reticle. The reticle radius was chosen to be  $1^\circ$  and the nutation radius was chosen to be  $0.6^\circ$ . This gives a total **FOV** of  $1.6^\circ$  as a radius or  $3.2^\circ$  as a diameter. The present analysis did not consider background clutter or flare countermeasures, only the target as the sole object in the field of view. These assumptions are believed to be reasonable as the **FOVs** are realistic, and the effects of the target and jammer can be analysed without interference from other sources.

A block diagram of the signal processing is shown in Fig. 3. The detector signal passes through an **automatic gain control (AGC)** system which adjusts the amplitude of the signal to a fixed magnitude for further processing (the information is contained in the frequency of the signal and not the signal's amplitude). The **AGC** circuit is implemented using an averaging circuit. The mean of



the previous scan cycle is used to determine the gain of the current detector amplitude. Depending on the missile type, the **AGC** may or may not be followed by a hard limiter. In this study we choose to not use a hard limiter in common with the majority of authors.<sup>8-13,21,22</sup> Note that because the effect of the saturation or hard limiting in electronic components were not modelled, the results obtained here assumed linearity and therefore represent the highest possible effect achievable with the specific jam codes. Initial experiments indicated that hard limiting substantially changes the effectiveness of the various jam codes. Jam codes for seekers with hard limiting requires more research.

The signal is then passed through a **band-pass filter (BPF)** which is centred at the nominal carrier frequency of 1.2 kHz to remove any low- and high-frequency background signals and noise. The carrier filter is centred at 1.6 kHz in the simulation, and not at the carrier frequency in order to extend the linear region of the static gain curve of the seeker, allowing a wider range of radial positions to be demodulated accurately.<sup>22,23</sup> The signal is then passed through a frequency discriminator which converts the **FM** signal to an **amplitude modulation (AM)** signal. The frequency discriminator is implemented using a **high-pass filter (HPF)** with a cut-off frequency of 1.8 kHz. The signal is then passed through an envelope detector which gives the envelope of the signal. The envelope detector is implemented using a full-wave rectifier and a **low-pass filter (LPF)** with a cut-off frequency of 100 Hz. The high-frequency components that are generated by rectification are filtered out by the **BPF** centred on the nutation frequency, and a phase detector is then used to determine the phase of the signal. The **BPF** is centred at the nutation frequency of 100 Hz with a bandwidth of 40 Hz to provide a reasonable quality estimate of the envelope. The phase detector is implemented using a second order polynomial fit to the data as a reference for the radial and angular position of the target.

The phase detector produces two outputs which represent the error (target displacement from the optical axis) in the pitch and yaw directions. These two error signals are used to steer the seeker gimbal optical axis towards the target. The Zeigler-Nichols Method was used for tuning the controller, and the gain of 0.7 was found to be the edge of stability.<sup>24</sup> This gain was therefore chosen for the proportional controller. The gain is applied to the error signals, steering the gimbal with proportional control. A proportional controller is used since this is the controller of choice in a number of simulations.<sup>8,11</sup> The gimbal rate is limited to  $1^\circ$  per nutation cycle in order to model the effect of the inertia of the gimbal assembly.

### **3 Jammer signal effect**

A conical-scan seeker simulation was developed to test jam signal effectiveness. The 12-spoke wagon wheel reticle shown in Fig. 2 was chosen for spatial filtering, and the signal processing block diagram as shown in Fig. 3. The seeker nutation frequency was set at 100 Hz, so the target takes 10 ms to move around its nutation circle. The combination of the 12-spoke wagon wheel reticle and a nutation frequency of 100 Hz result in a carrier frequency of  $100 \times 12 = 1.2$  kHz. The detector signal is generated by multiplying the reticle image by the target source image which is nutated at an angular step-size of  $1^\circ$  on the reticle, resulting in 360 samples per nutation period of 10 ms. The nutation radius was chosen to be  $0.6^\circ$  whereas the reticle radius was chosen to be  $1^\circ$ . The area outside of the reticle is considered opaque and the detector can therefore not detect the target beyond the boundary of the reticle. The point at which the outside of the nutation path touches the outer edge of the reticle is the edge of the total FOV. In this case, the edge of the FOV is  $1.6^\circ$ . The total FOV can also be given as a diameter, which is  $3.2^\circ$  in this case. The parameters used in the demodulation process are given in Fig. 3. The simulation model output was compared

to results from other simulations systems.<sup>8,11,23</sup> The time taken for the model to reduce specified errors to zero was considered. The fixed carrier jam signal is generally used in the literature for jam signal analysis and this jam signal was used in this study for validation.<sup>8,11</sup> The effect of varying the *J/S* ratio and the carrier frequency of a jam signal was compared with the literature with satisfactory results.<sup>23</sup>

The seeker was set up to track target movement with an angular position loop; for a stationary target there should be no change in seeker angular position. The simulation attempts to measure the countermeasure effectiveness by testing for an erroneous apparent seeker position, attributable only to the countermeasure presence, when viewing a stationary target. If the apparent position of the target is driven outside of the seeker *FOV*, *OBL* is declared.

The simulation work flow is as follows: (1) The target is inertially stationary in the sense that its relative angular position does not change with time. (2) The target is placed on the optical axis (the target's nutation circle falls on the centre of the reticle). (3) The seeker is exposed to the target signal only, for 30 ms during which the transient effects are expected to die out. (4) The jammer signal is switched on and the tracking error induced in the seeker is measured for a period of 300 ms. (5) The tracking behaviour in the first 200 ms is ignored (to avoid transient oscillations). (6) The maximum error achieved after 200 ms is used as a measure of jammer effect.

The simulation was used to test a number of different jam-code parameters to determine the effect of these parameters on the seeker. The parameters that were considered when designing jammer waveforms were the carrier frequency and the envelope amplitude as shown in Fig. 4 and Table 1.

The combination of the carrier frequency and the envelope amplitude was used to characterise the jam signals that were tested. The target signal as a source consists of a constant amplitude and

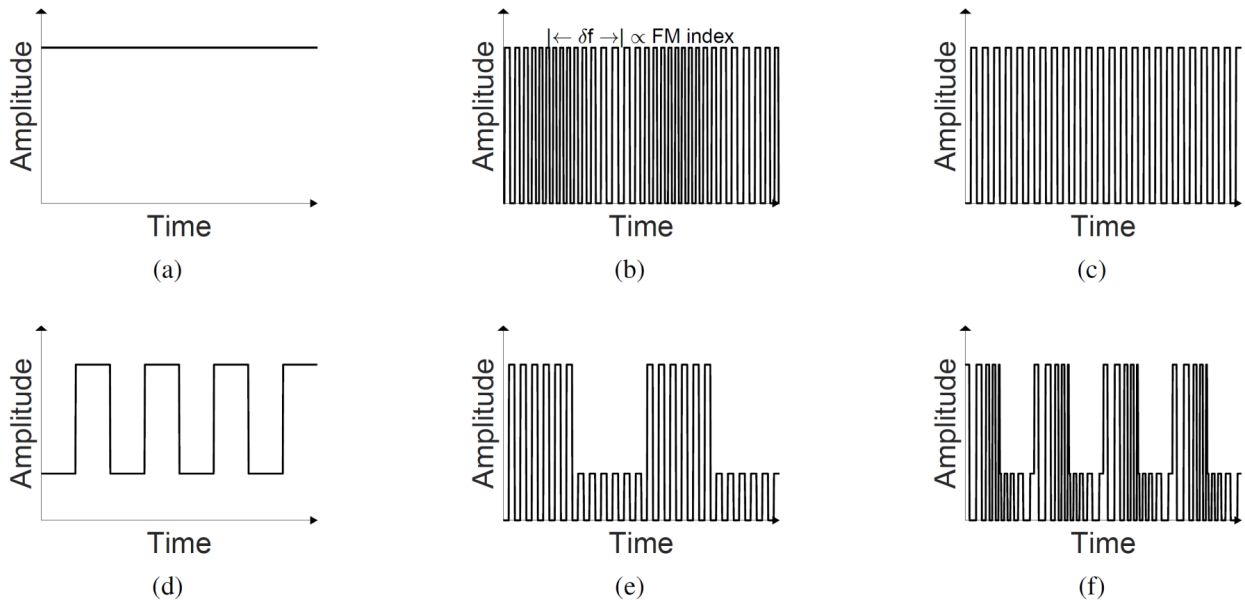


**Fig 4** Catalogue of target and jamming signals. (a) Target, (b) fixed carrier, (c) FM, (d) low frequency, (e) AM and (f) AM-FM hybrid jam signals.

**Table 1** Types of jammer waveforms and their characteristics.

Envelope	Carrier		
	Baseband (No carrier)	Constant frequency	Variable frequency
Constant amplitude	Target	Fixed carrier	FM
Variable amplitude	Low frequency	AM	AM-FM hybrid

no carrier. The fixed carrier jam signal consists of a constant amplitude and a constant frequency (with the frequency range close to the seeker carrier frequency). The FM jam signal consists of a constant amplitude with a varying carrier frequency. The FM jam signal is assumed to have a repetition rate or modulation frequency that is equal to the nutation period or frequency respectively. The low frequency jam signal consists of a variable amplitude and no carrier signal. The low frequency jam signal oscillates at a frequency close to the seeker nutation frequency. The AM jam signal consists of a variable envelope amplitude with a fixed carrier frequency. The hybrid AM-FM jam signal, varies in the envelope amplitude and consists of a variable carrier frequency. Since the study is a fundamental study to understand the basics of what makes a jam code effective,

the hybrid AM-FM jam signal was not tested due to its complexity.

### 3.1 Effect of the J/S ratio and frequency

The literature suggests that an increase in the J/S ratio causes an increase in the jammer effect.<sup>6,8-13</sup> This statement was tested and results shown in Fig. 5. OBL occurs at 1.6° in the seeker under study since the seeker total FOV is 3.2°.<sup>21</sup>

Most studies<sup>8-13</sup> consider J/S ratios from 1 to 10, but modern DIRCM systems are capable of higher J/S ratios. The J/S ratios that were considered range from 2 to 100.<sup>25</sup> Note, again, that the effect of the saturation in electronic components was not modelled and therefore the effect shown in each figure represents the highest possible effect achievable with the specific jam code. These jam codes will cause different results in a seeker with saturation or hard limiting.

As seen in Fig. 5, the jam code effect increases as the J/S ratio increases, in agreement with the literature.<sup>6,8-13</sup> However, the effectiveness of each jam code considered saturates at some point. In the case of the fixed carrier jam code shown in Fig. 5 (a), the effect of the jam code does not significantly increase beyond a J/S ratio of 10, even if saturation of electronic components is not considered. It can be seen in the figure that the jam signal has a greater effect for jam code frequencies between 1.3 kHz to 1.6 kHz. Remember that the carrier BPF used in the processing circuit (see Fig. 3) is centred at 1.6 kHz with a bandwidth of 500 Hz. The logical conclusion is that the jamming effect increases for jamming frequencies in the processing BPF bandwidth. The frequency discriminator used in the processing block (see Fig. 3) consists of a HPF with a cut-off frequency of 1.8 kHz. This HPF is the reason for jam frequencies below 1.2 kHz showing minimal effect. If a LPF was used in the discriminator, the jam effect seen in Fig. 5 (a) would be inverted about the carrier frequency of 1.6 kHz. This is an example of how the effect of a jam signal is

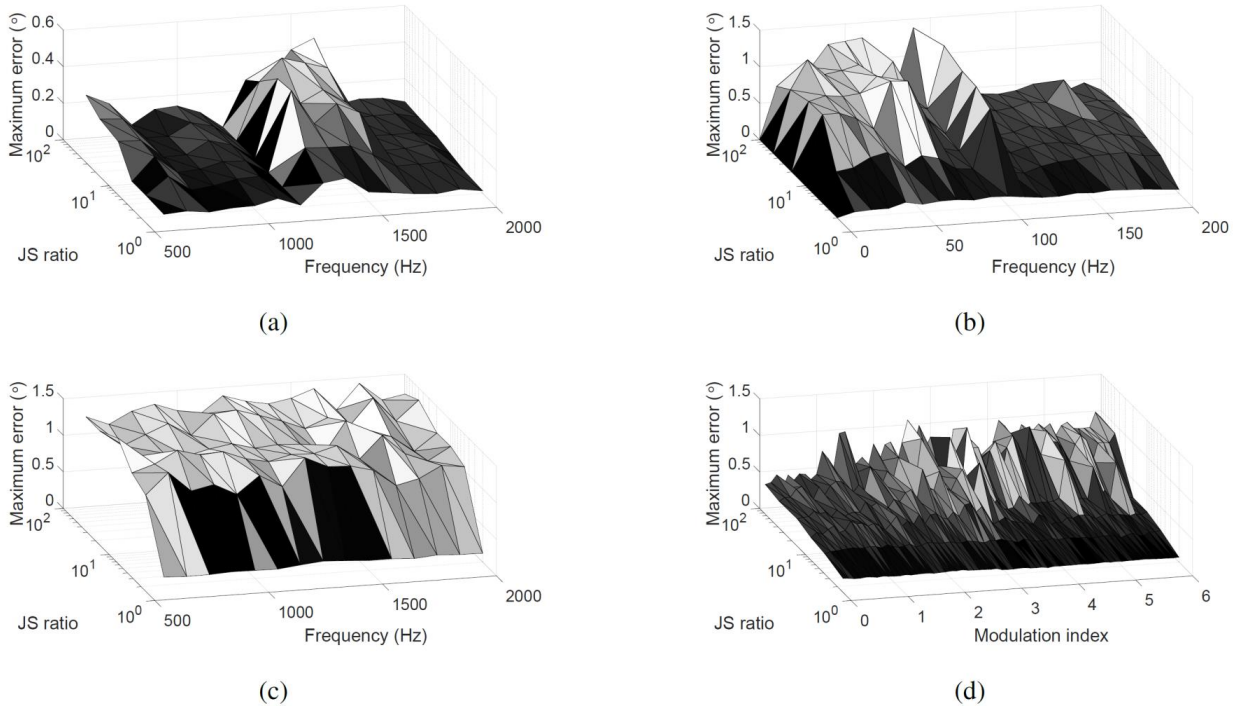


**Fig 5** Effect of  $J/S$  ratio and jammer frequency for the (a) fixed carrier, (b) low frequency, (c) **AM** with carrier and (d) **FM** jam codes.

dependent on the signal processing used to demodulate the detector signal. It was observed that the jam signal effectiveness is zero for a jam frequency of 1.2 kHz. In this case, the jam signal will act as a beacon, making it easier to track the target.

In the case of the low-frequency jam signal shown in Fig. 5 (b), the greatest effect is achieved at jam frequencies in the vicinity of 50 Hz and 100 Hz. Setting the jammer frequency to coincide with the nutation frequency allows this type of jam signal to illuminate the reticle at the same angle in each nutation cycle creating a consistent error in the processor. The same argument can be used for the effect that is seen at a frequency of 50 Hz which illuminates the reticle at the same angle every second nutation cycle. With this type of jam signal, the error induced increases with an increase in the  $J/S$  ratio, but beyond a  $J/S$  ratio of 10 there is no significant increase.

The effect of the **AM** jam signal is shown in Fig. 5 (c). The jam effect increases significantly with a  $J/S$  ratio increase from 2 to 5, but the effect does not increase with a further increase in the

$J/S$  ratio. The **AM** jam signal produces a similar effect for all the carrier frequencies considered in the experiment. This means the jam signal has a low sensitivity to the carrier frequency. This can be advantageous when countering a conical-scan seeker with an unknown carrier frequency or signal processing filter frequency. The **AM** jam signal is effective for a wider range of frequencies than the other jam signals that were considered in the experiment.

The **FM** jam signal was tested for modulation indices ranging from 0.1 to 6 with a base frequency of 1.2 kHz. As a general guide, the modulation index should be close to unity for laser efficiency and therefore the maximum modulation index was limited to 6.<sup>7</sup> The maximum modulation index of 6 causes the carrier frequency to vary from 600 Hz to 1.8 kHz each nutation cycle. The results of the **FM** jam signal are shown in Fig. 5 (d). As seen in the figure, the jam signal is not effective for modulation indices below 2. The jam signal is effective at other indices, but the effect varies significantly with even small changes in the modulation index. This is a disadvantage since a slight change in the carrier frequency could result in a significant change in the jam signal effectiveness.

A sensitivity analysis was conducted to analyse the effect of slight changes in the carrier frequency or carrier modulation index. The standard deviation was used as a measure of sensitivity since it gives the deviation of the data from the mean of the data. The sensitivity was tested for the highest  $J/S$  ratio only. The sensitivity for the fixed carrier jam signal was found to be  $0.13^\circ$  which is 8% of the total **FOV**. This means the seeker error will deviate by a maximum of 8% from the mean error achieved by this jam signal with a change in the carrier frequency. It is obviously desirable to have the lowest sensitivity, since this will mean changes in the carrier frequency or modulation index will cause minimal change to the seeker error achieved by the jam signal. The sensitivity of the low-frequency jam signal was found to be  $0.39^\circ$  which is 24% of the total **FOV**. This is

significantly higher than the sensitivity of the fixed carrier jam signal. This can be confirmed by observing the changes in the seeker error with a change in the frequency in Fig. 5 (b). The sensitivity for the AM jam signal was found to be  $0.1^\circ$  which is 6.2% of the total FOV. This is the lowest sensitivity obtained across all the jam signals. The FM jam signal produced a sensitivity of  $0.22^\circ$  which is 14% of the total FOV. While the FM jam signal produces the highest number of oscillations in its effectiveness, the low-frequency jam signal produces the highest sensitivity overall to changes in the carrier frequency. Even though the FM jam signal changes in effect with changes in modulation index, the variations are not as large as the variations found in the low-frequency jam signal.

Note that none of the jam signals considered in the experiment produce OBL, even for J/S ratios as high as 100. This is most likely due to the target and seeker being stationary, which makes the tracking of the target much easier. The jam effect would cause greater disturbance for a moving target, and OBL would be easier to achieve.

### 3.2 *Effect of modulation frequency*

In the case of the AM and FM jam signals, the waveform consists of a carrier signal and an envelope or modulation signal. In the previous section, the effect of varying the carrier frequency of these waveforms was tested. In this section the effect of varying the modulation frequency is described with the results shown in Fig. 6. The highest J/S ratio of 100 is used for the jam signals tested in this section.

In the case of the AM jam signal, the carrier frequency was fixed at 1.8 kHz, and the modulation frequency varied from 50 Hz to 150 Hz (results shown in Fig. 6 (a)). A carrier frequency of 1.8 kHz was chosen since this is the carrier frequency at which the highest effect was achieved for a J/S



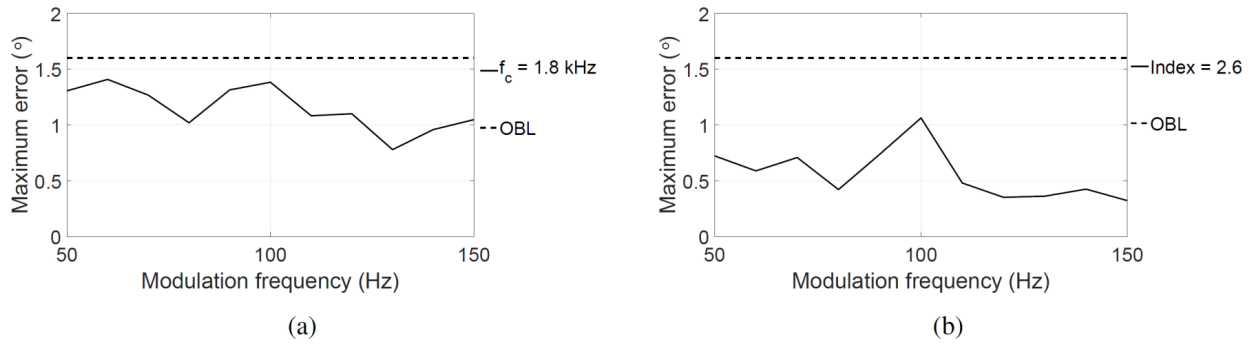


**Fig 6** Effect of the modulation frequency for the (a) 1.8-kHz AM jam signal and (b) FM jam signal with a modulation index of 2.6.

of 100. As seen in the figure, the AM jam signal is not significantly affected by a change in the modulation frequency. The jam effect increases from  $1.31^\circ$  to  $1.38^\circ$  as the modulation frequency changes from 90 Hz to 100 Hz, but then decreases to  $1.1^\circ$  as the modulation frequency is increased to 110 Hz. The greatest jam effect is achieved at 60 Hz and 100 Hz. The sensitivity of the jamming effect to changes in the modulation frequency is  $0.2^\circ$ , which is 12.5% of the total FOV.

In the case of the FM jam signal, shown in Fig. 6 (b), the jam effect against modulation frequency was tested with the modulation index fixed at 2.6. This was the best performing index for a  $J/S$  of 100. As seen in Fig. 6 (b), the jam effect changes significantly with a slight change in the modulation frequency. If the modulation frequency changes from 100 Hz to 90 Hz, the effect reduces from  $1^\circ$  to  $0.42^\circ$ , while an increase from 100 Hz to 110 Hz causes a decrease in effect from  $1^\circ$  to  $0.48^\circ$ . The sensitivity of this jam signal to changes in the modulation frequency is  $0.23^\circ$  which is 14.3% of the total FOV. The sensitivity of the FM jam signal to changes in modulation frequency is higher than that of the AM jam signal in this experiment. The greatest effect is achieved at a modulation frequency of 100 Hz for the FM jam signal. The best jamming effect in most cases occur near the nutation frequency.

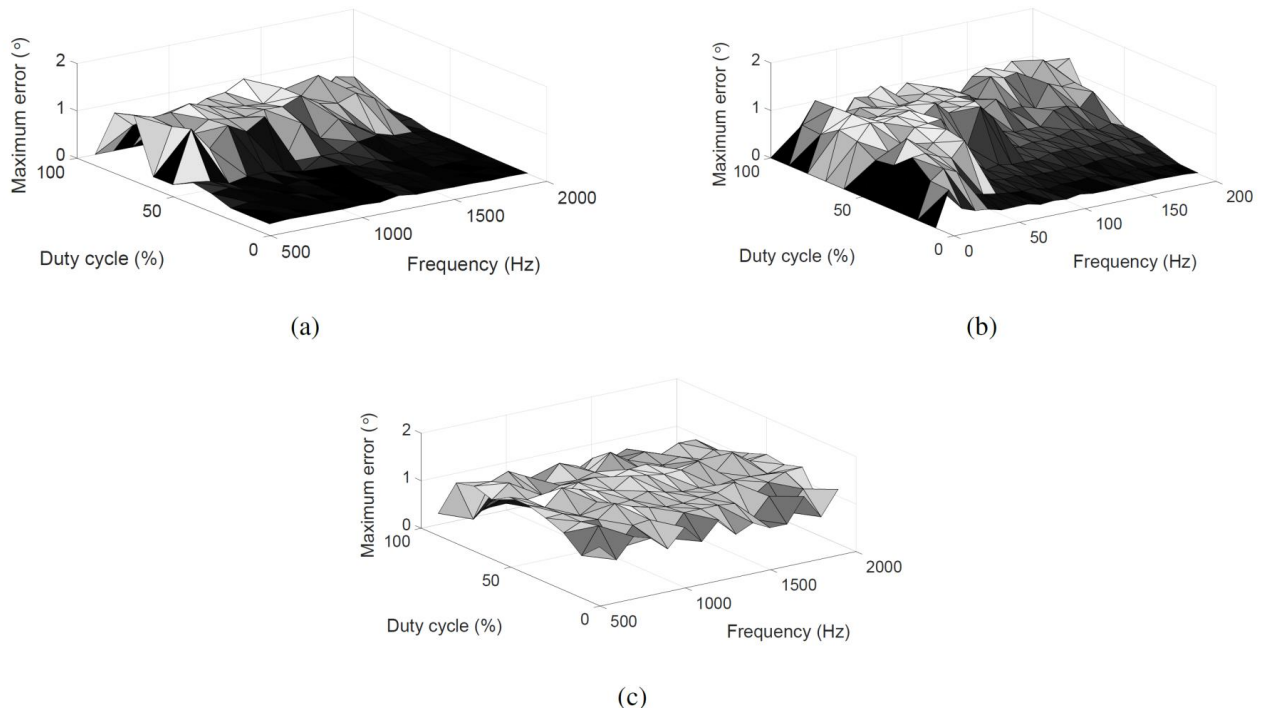


**Fig 7** Effect of the duty cycle for the (a) fixed carrier, (b) low-frequency, and (c) AM jammers.

### 3.3 Effect of the duty cycle

The duty cycle determines the percentage of time that a jam signal will be switched on during its cyclic period. In the tests conducted for the J/S ratio, and frequency, all the jam signals were operating at a duty cycle of 50%. In order to test the effect of varying the duty cycle, each jam signal was set at a J/S ratio of 100. The frequency was then swept from 600 Hz to 2 kHz in the case of the fixed carrier and the AM jam signals; and from 0 Hz to 200 Hz in the case of the low frequency jam signal, keeping the duty cycle constant. The sweep was conducted for each duty cycle. The effect of the duty cycle across the operating frequencies of the jam signal is shown in Fig. 7. The effect of the duty cycle was tested for the fixed carrier, low-frequency, and the AM jammer waveforms. The effect of the duty cycle for the FM jam signal was not tested because it naturally consists of a variable duty cycle.

In the case of the fixed carrier jam signal, the carrier duty cycle was varied for the range 600 Hz

to 2 kHz, and the maximum error achieved is presented in Fig. 7 (a). As seen in the figure, the jam effect is insignificant at duty ratios below 60% across all the frequencies. The effect increases slightly in the range 60% to 90%, and the effect is zero at a 100% duty cycle. At a 100% duty cycle the jamming effect produces a **direct current (DC)** signal with a fixed carrier jam signal, leading to a  $0^\circ$  error in the seeker. It can be concluded that it is more energy efficient to operate at a duty cycle of 60% since an increase in duty cycle beyond the 60% mark does not produce a significant increase in jam effect. In the case of the low-frequency jam signal, the frequency was varied in the range 0 Hz to 200 Hz for each duty cycle, and the maximum error achieved for each duty cycle is shown in Fig. 7 (b). As seen in the figure, the effect of the duty cycle is not consistent for all the frequencies. At the higher range of frequencies, the jam effect is generally lower for low duty cycles. In general the jam effect increases with an increase in the duty cycle. Beyond 50% the jam effect does not improve with an increase in duty cycle. The jam effect completely dies out at a duty cycle of 100% in the low-frequency case due to the signal being a **DC** signal.

In the case of the **AM** jam signal, the envelope duty cycle was tested with the duty cycle of the carrier signal kept at a constant 50%. The carrier frequency was varied from 600 Hz to 2 kHz for each duty cycle, and the maximum error achieved in each duty cycle is shown in Fig.7 (c). As seen in the figure, an increase in the duty cycle in the range 10% to 80% does not significantly change the jam effect of the **AM** jam signal. The effect significantly decreases as the duty cycle increases from 80% to 100%. These results suggest that it would be advantageous to operate in the 10% to 60% range in the case of the **AM** jam signal. Note that the **AM** jam signal produces a greater effect at a duty cycle of 10% than the other jam signals, making this jam signal the most energy efficient.

A sensitivity analysis was conducted to measure the effect of changes in the duty cycle for each jam signal. The fixed carrier jam signal produced a sensitivity of  $0.54^\circ$  (33.8% of total **FOV**). The

low-frequency produced a sensitivity of  $0.44^\circ$  (27% of total FOV) while the AM signal produced a sensitivity of  $0.29^\circ$  (18% of the total FOV). As expected, the highest sensitivity to changes in the duty cycle was found in the fixed carrier jam signal. This corresponds with what is seen in Fig. 7 (a).

Since the tests conducted on the J/S ratio and the frequency were conducted at a duty ratio of 50%, the fixed carrier jam signal did not seem to be effective. The duty cycle tests showed that the fixed carrier jam signal can be effective if the duty cycle is greater than or equal to 60%. This shows how the jam effect is dependant on multiple factors, so it is not sufficient to consider one parameter in isolation. This means it cannot be concluded that the fixed carrier jam signal is effective for the frequencies shown previously in Fig. 7 (a), unless the duty cycle and J/S ratio under which those results were obtained is known.

### 3.4 Jam signal effect analysis

A summary of the findings for each jam signal is shown in Table 2. For comparison purposes, a jam signal was considered effective if it achieves an error greater than or equal to  $1.6^\circ$  in the first section of the table for each parameter tested. This is the point at which OBL occurs. Since none of the jam signals tested in the experiment could achieve OBL, the second section of the table compares the jam signals against a seeker error of  $1^\circ$  since this is the edge of the reticle. The parameters were compared at a J/S ratio of 100 to ensure that all of the jam signals achieve their maximum effect. The modulation frequency was fixed at the nutation frequency of 100 Hz unless otherwise stated. The duty cycle was varied in order to find the best and worst case as required for each parameter.

The maximum error achieved for a J/S ratio of 100 for each jam signal is given as the first

**Table 2** Summary of jam signal effectiveness. Some combinations are **not applicable (N/A)**.

Parameter	Fixed carrier	Low frequency	AM	FM
<b>Jam effectiveness: 100% represents a 1.6° induced track error</b>				
Maximum error for J/S = 100 [%]	77.3	87.9	90.0	66.3
Sensitivity to carrier frequency or index ( $\sigma$ ) [%]	25.0	N/A	20.0	14.0
Sensitivity to modulation frequency ( $\sigma$ ) [%]	N/A	25.0	15.2	14.3
Sensitivity to duty cycle ( $\sigma$ ) [%]	33.7	27.3	18.0	N/A
<b>Jam code parameter ranges of most effective jamming</b>				
Minimum required J/S ratio	10 (80% duty cycle)	5 (60% duty cycle)	5 (50% duty cycle)	50
J/S ratio required for maximum error	100	100	50	50
Effective carrier frequency [kHz]	0.6 to 1.1 (80% duty cycle)	N/A	0.6 to 2.0 (50% duty cycle)	N/A
Effective carrier modulation index	N/A	N/A	N/A	2.6
Effective modulation frequency [Hz]	N/A	40 to 60, 90 and 100	50 to 110	100
Effective duty cycle [%]	60 to 90	30 to 90	10 to 90	N/A

parameter in Table 2. The low frequency and AM jam signals produce approximately similar highest error of 1.4° (87.9%) and 1.44° (90%) respectively.

The sensitivity of each jam signal to variations in the carrier frequency or the carrier modulation index is given as the next parameter. The standard deviation was again used as a measure of sensitivity for each parameter tested. The carrier frequency was varied from 600 Hz to 2 kHz with the duty cycle fixed at 10%. The standard deviation of the error was then recorded. The duty cycle was incremented to 20% and the frequency sweep was conducted again. This process was continued until the standard deviation was computed for all the duty cycles. The highest standard deviation achieved across all the duty cycles was then taken as the worst case sensitivity.

It was found that the FM jam signal is the least sensitive to frequency changes in the index with a standard deviation of  $0.2^\circ$  (14%). This means the FM jam signal error deviates the least from the mean value. In the analysis conducted in Section 3.1, the AM jam signal had shown the lowest sensitivity of 6.2% to carrier frequency, but this was at a duty cycle of 50%. Since the sensitivity is now considered across all the possible duty cycles for the low-frequency and AM jam signals, the maximum sensitivity is now seen. This shows how critical the duty cycle is when assessing jam signal effectiveness.

In order to test the sensitivity of the jam signals to changes in the modulation frequency, the carrier frequency or index had to be fixed in the case of the AM and FM jam signals. The carrier frequency for the AM jam signal was fixed at 1.8 kHz and the modulation index in the FM case was fixed at 2.6. These were chosen since the greatest seeker error was achieved at these settings. In the case of the low frequency and AM jam signals, the modulation frequency was varied at different duty cycles and the highest sensitivity observed is shown in the table. It was found that the FM jam signal showed the least sensitivity to changes in the modulation frequency with a standard deviation of  $0.23^\circ$  (14.3%). The analysis conducted on modulation frequency in Section 3.2 produced a sensitivity of 12.5% for the AM signal and 14.3% for the FM jam signal. Since the analysis given here was conducted at all the duty cycles, an overall sensitivity to modulation frequency is seen. This shows the significant effect the duty cycle has on jam effectiveness in terms of the modulation frequency as well.

The sensitivity of each jam signal to changes in duty cycle is given next. The AM jam signal is the least sensitive to variations in the duty cycle with a standard deviation of  $0.29^\circ$  (18%). The fixed carrier jam signal is the most sensitive to change in the duty cycle with a standard deviation of  $0.54^\circ$  (33.7%) – almost twice that of the AM jam signal.

Since none of the jam signals could achieve OBL in the conducted experiment, the jam signals are compared against an error of  $1^\circ$ , the edge of the reticle. The minimum J/S ratio that could successfully achieve an error greater than or equal to  $1^\circ$  is the next compared parameter. Jam effectiveness changes with a change in the duty cycle, so the duty cycle at which the greatest error could be achieved is given in brackets in the table. The FM jam signal requires the highest J/S ratio of 50 to achieve an effect of  $1^\circ$ , making it the most power intensive. The low-frequency and AM jam signals require the lowest J/S ratio of 5 to be effective.

The next compared parameter is the J/S ratio at which maximum seeker error could be achieved. This test was conducted at a duty cycle of 50% with a fixed modulation or envelope frequency for the fixed carrier, AM and FM jam signals. The modulation frequency was variable in the case of the low-frequency jam signal. The carrier frequency or carrier modulation index was varied in the test. The general guide provided in literature suggests that the highest J/S ratio should produce the greatest seeker error.<sup>6,8-13</sup> As seen in the table, the maximum error for the AM and FM jam signals were not achieved at the highest J/S ratio of 100. The effect achieved at a J/S ratio of 100, and that achieved at a J/S ratio of 50 for the AM case, is equal. In the case of the FM jam signal, the effect achieved at a J/S ratio of 100 is lower than that achieved at a J/S of 50. This finding shows that the required J/S ratio does not necessarily have to be the maximum available setting, it should be judged per individual case.

Next consider the range of carrier frequencies for which each jam signal was effective at a J/S ratio of 100. A change in duty cycle has an effect on the jam signal frequency response, therefore, the duty cycle at which the greatest error is achieved is provided in brackets. The AM jam signal is effective for the widest range of carrier frequencies with a range of 600 Hz to 2 kHz, with the FM jam signal being effective at only a single modulation index.

The effect of modulation frequency is then considered. Both the AM and low-frequency jam signals are effective for a wide range of modulation frequencies. The FM jam signal is effective at only one modulation frequency which is equal to the nutation rate.

The range of effective duty cycles is the next compared parameter in the table. The AM jam signal produces a significant error for the majority of duty cycles. This jam signal is the only signal to produce a significant effect at the lowest duty cycle of 10% and this makes it the most power efficient.

The general guide provided in the literature,<sup>6,8-11,13</sup> suggests that the carrier frequency should be close to the target generated carrier frequency. The results in the table show that the effective carrier frequency varies depending on the type of jam signal used. This is due to the difference in interaction that each jam signal has with the target signal resulting in a different overall signal in the detector. Contradictory to what is generally published in the literature,<sup>6,8-13</sup> it was found that the jam signal does not necessarily achieve maximum effect at the maximum J/S. The effect of duty cycle is hardly considered in the majority of studies.<sup>6,8-12</sup> In the analysis conducted here, the duty cycle has a major effect on jam signal effectiveness. While the AM jam signal produces good results for some duty cycles, the effect is not the same for other duty cycles. This means knowing the jam signal type that can be used is not sufficient. The duty cycle at which the jam signal is operated is a crucial part of selecting the jam signal. The analysis of jam signal effectiveness is a complex task and requires multiple factors to be considered in the analysis. The use of optimisation algorithms could provide better insight on the optimal matching of jam signal parameters for maximum jam success.

The results in Table 2 show that the AM and low-frequency jam signals have the highest error at a J/S ratio of 100, require the lowest J/S ratio to achieve an error of 1°, have the widest range



of effective carrier and modulation frequencies, have the widest range of effective duty cycles, achieve significant errors at the lowest duty cycles and have the lowest sensitivity to duty cycle. In light of these results, it appears that **AM** and low-frequency jam signals have the greatest potential to effectively counter conical-scan frequency-modulated seekers with wagon-wheel reticles, given that the best duty cycle is chosen.

#### 4 Conclusion

Four types of jammer waveforms were investigated in order to assess the parameters that ensure success of jamming of conical-scan frequency-modulated seekers with wagon-wheel reticles. These waveforms are the fixed carrier, low-frequency, **AM**, and **FM** jam signals. The jam signal parameters that were tested are the **J/S** ratio, carrier and modulation frequencies, and the duty cycle.

Contrary to the general guide provided in the literature,<sup>6,8-11,13</sup> it was found that the jam signal carrier frequency does not necessarily have to be close to the target carrier frequency for maximum jam signal effect. This is due to the difference in interaction each jam signal has with the target signal, producing different detector responses. The maximum error achieved in the experiment for the **AM** and **FM** jam signals was not achieved at the maximum **J/S** ratio of 100, as suggested in the literature.<sup>6,8-13</sup> This indicated that each jam signal should be individually tested for jam effectiveness. The effect of the duty cycle proved this parameter critical in jam signal effectiveness. For each jam signal waveform considered, the greatest jam signal effect was achieved at different duty cycles.

The jam signals that were tested did not produce **OBL** in the simulated seeker, even for high **J/S** ratios. This is probably a result of the target and reticle positions not changing during the

experiments, making the tracking process simpler than it would be for a real engagement.

While an increase in the *J/S* ratio was found to produce an increase in the seeker error, the effect of increasing the *J/S* ratio saturates at a value which differs for each jam signal. The effect of the remaining parameters was found to vary depending on the jammer signal considered.

The *AM* jam signal produces a large tracking error and has low sensitivity to parameter variations when used against a conical-scan frequency-modulated seeker with a wagon-wheel reticle, making it the most promising of the jam signals considered.

### *References*

- 1 W. Taylor, "Protecting civil aircraft from the manpad threat: is this a practical scenario?," *Technologies for Optical Countermeasures II* (2005).
- 2 J. R. Bartak, "Mitigating the MANPADS threat: international agency, US, and Russian efforts," Master's thesis, Naval Postgraduate School, Monterey, USA (2005).
- 3 D. H. Titterton, "A review of the development of optical countermeasures," in *Proc. SPIE*, **5615**(1) (2004).
- 4 F. Neri, *Introduction to Electronic Defense Systems*, Artech House radar library, SciTech Publishing, Incorporated (2006).
- 5 C. R. Smith, R. Grasso, J. Pledger, *et al.*, "Trends in electro-optical electronic warfare," *Proc. SPIE* **8543**, 8543 – 8543 – 17 (2012).
- 6 J. R. White, *Aircraft Infrared Principles, Signatures, Threats, and Countermeasures Handbook.*, Naval Air Warfare Center Weapons Division, California (2012).

- 7 B. Molocher, “Countermeasure laser development,” in *SPIE Technol. Opt. Countermeasures II; Femtosecond Phenomena II; and Passive Millimetre-Wave and Terahertz Imaging II*, **5989**, 16–25, (Bruges, Belgium) (2005).
- 8 T. W. Bae, B. I. Kim, Y. C. Kim, *et al.*, “Jamming effect analysis of infrared reticle seeker for directed infrared countermeasures,” *Infrared Phys. Technol.* **55**, 431–441 (2012).
- 9 C. J. Tranchita, K. Jakstas, and R. G. Palazzo, “Countermeasure systems,” in *The Infrared & Electro-Optical Systems Handbook*, D. H. Pollock, Ed., **7**, ch. 3, 235–285, ERIM and SPIE Press, Raleigh, USA (2006).
- 10 T. L. Chang, “The IR missile (spin-scan and con-scan seekers) countermeasures,” Master’s thesis, Naval Postgraduate School, Monterey, USA (1994).
- 11 G. Y. Kim, B. I. Kim, T. W. Bae, *et al.*, “Implementation of a reticle seeker missile simulator for jamming effect analysis,” in *Int. Conf. Image Process. Theory Tools Appl.*, 539–542, (Paris, France) (2010).
- 12 F. Qian, J. Guo, J.-F. Shao, *et al.*, “Study of jamming of the frequency modulation infrared seekers,” in *SPIE Int. Symp. Photoelectronic Detection Imaging; Infrared Imaging Appl.*, 28–36, (Beijing, China) (2013).
- 13 M. C. Sahingil and M. S. Aslan, “The effectiveness of the jammer signal characteristics on conical-scan systems,” in *SPIE Conf. Modelling Simulation Defence Syst. Appl.*, 86–101, (Baltimore, USA) (2015).
- 14 C. J. Willers and M. S. Willers, “Simulating the dircm engagement: component and system level performance,” *Proc. SPIE* **8543**, 8543 – 8543 – 16 (2012).
- 15 W. L. Wolfe and G. Zissis, *The Infrared Handbook*, Office of Naval Research, US Navy,

- Infrared Information and Analysis Center, Environmental Research Institute of Michigan (1978).
- 16 R. D. Hudson, *Infrared System Engineering*, Wiley-Interscience, New York (1969).
  - 17 J. M. Shima, "Fm demodulation using a digital radio and digital signal processing," Master's thesis, University of Florida (1995).
  - 18 A. J. Noga, "Numerical FM Demodulation Enhancements," Technical Report RL-TR-96-91, Rome Laboratory, US Air Force Materiel Command (1996).
  - 19 Z. W. Chao and J. L. Chu, "Digital simulation of frequency modulation reticles," *Optical Engineering* **29**, 68–84 (1990).
  - 20 J. S. C. Sung-Hyun Han, HyunKi Hong, "Dynamic simulation of infrared reticle seekers and an efficient counter-countermeasure algorithm," *Optical Engineering* **36**, 36 – 36 – 5 (1997).
  - 21 R. P. Birchenall, M. Richardson, B. Brian, *et al.*, "Modelling an infrared man portable air defence system," *Infrared Phys. Technol.* **53**, 372–380 (2010).
  - 22 J. Jackman, *Pre-Emptive Infrared Countermeasures*. PhD thesis, Cranfield Defence And Security (2011).
  - 23 T. M. Malatji and W. du Plessis, "Jammer signal effectiveness against a conical-scan missile seeker," in *Africon*, 591 – 596, (Cape town, South Africa) (2017).
  - 24 W. Altman and D. MacDonalds, *Practical Process Control for Engineers and Technicians*, ch. Tuning of PID controllers in both open and closed loop control systems, 112 – 130. Oxford (2005).
  - 25 D. H. Titterton, *Development of Infrared Countermeasure Technology and Systems*, 635–671. Springer, London, UK (2006).

**Tsholofelo M. Malatji** received the B.Eng. (Electronic) and B.Eng. (Hons) (Electronic) degrees from the University of Pretoria in 2013 and 2017 respectively. She obtained Golden Key status during undergraduate studies and completed the B.Eng. (Hons) degree with distinction. She was employed by the national power producer Eskom in the year 2014, where she was employed as a power line design engineer. She was then employed as an Infrared Electronic Warfare (IREW) researcher in the Optronics Sensor Systems Competency (OSS) department at the Council for Scientific and Industrial Research (CSIR) from the year 2017, where her research focus is platform protection, modelling and simulation and jamming. She is currently employed at the CSIR and conducting her M.Eng. studies with the University of Pretoria.

**Warren P. du Plessis** received the B.Eng. (Electronic) and M.Eng. (Electronic) and Ph.D. (Engineering) degrees from the University of Pretoria in 1998, 2003 and 2010 respectively, winning numerous academic awards including the prestigious Vice-Chancellor and Principal's Medal. He spent two years as a lecturer at the University of Pretoria, and then joined Grintek Antennas as a design engineer for almost four years, followed by six years at the [Council for Scientific and Industrial Research \(CSIR\)](#). He is currently an Associate Professor at the University of Pretoria, and his primary research interests are cross-eye jamming and thinned antenna arrays.

**Cornelius J. Willers** completed a B.Sc. (Honours) Electronics Engineering at the University of Pretoria in 1976 and a MS (Optical Engineering) at the University of Arizona in 1983. He is registered as a professional (chartered) engineer. His 40 years work experience includes electro-optical system development, system architecture and systems engineering, software development, infrared signature modelling, and simulation. His most notable achievements include being the architect and technical lead in the establishment of imaging infrared missile seeker head technology, and

in the process, spearheading advanced physics-based image simulation. He published a 500-page book on electro-optical system design with SPIE Press in April 2013.

## List of Figures

- 1 Conical scan optics concept.
- 2 Typical wagon wheel reticle (a) with no error, and (b) the associated detector signal, (c) the wagon wheel reticle with a nutation error and (d) the associated detector signal.
- 3 Signal processing block diagram.<sup>20</sup>
- 4 Catalogue of target and jamming signals. (a) Target, (b) fixed carrier, (c) FM, (d) low frequency, (e) AM and (f) AM-FM hybrid jam signals.
- 5 Effect of J/S ratio and jammer frequency for the (a) fixed carrier, (b) low frequency, (c) AM with carrier and (d) FM jam codes.
- 6 Effect of the modulation frequency for the (a) 1.8-kHz AM jam signal and (b) FM jam signal with a modulation index of 2.6.
- 7 Effect of the duty cycle for the (a) fixed carrier, (b) low-frequency, and (c) AM jammers.

## List of Tables

- 1 Types of jammer waveforms and their characteristics.
- 2 Summary of jam signal effectiveness. Some combinations are N/A.